Ph.D. Program in Nanoscience and Technology (International)[1], Graduate School; Department of Food and Pharmaceutical Chemistry[2], Faculty of Pharmaceutical Sciences; Metallurgy and Materials Science Research Institute[3], Chulalongkorn University, Thailand

Curcumin diethyl disuccinate encapsulated in chitosan/alginate nanoparticles for improvement of its *in vitro* cytotoxicity against MDA-MB-231 human breast cancer cells

S. Bhunchu[1], C. Muangnoi[2], P. Rojsitthisak[1,3], P. Rojsitthisak[2],

Received June 29, 2016, accepted August 29, 2016

Pranee Rojsitthisak, Metallurgy and Materials Science Research Institute, Chulalongkorn University, Bangkok 10330, Thailand
pranee.l@chula.ac.th

Pharmazie 71: 691–700 (2016) *doi: 10.1691/ph.2016.6105*

Curcumin diethyl disuccinate (CDD) is a succinate prodrug of curcuminoids that has better stability in human plasma and improved *in vitro* cytotoxicity compared to curcumin. Therefore, CDD has the potential for further development as an anticancer agent. In this study, we focused on optimization of the formulation of CDD-loaded chitosan/alginate nanoparticles using Box-Behnken statistical design to enhance the therapeutic efficacy of CDD. Oil-in-water emulsification followed by ionotropic gelification was used to prepare the CDD-loaded chitosan/alginate nanoparticles. A formulation with a 0.05:1 chitosan/alginate mass ratio, 0.65% (w/v) Pluronic F127 and 1.5 mg/ml CDD was found to be optimal. FTIR, TGA and XRD confirmed the encapsulation of CDD molecules in the nanoparticles. *In vitro* cytotoxicity and cellular uptake studies showed that CDD-loaded chitosan/alginate nanoparticles had significantly higher cytotoxicity and cellular uptake in human breast adenocarcinoma MDA-MB-231 cells, compared to free CDD. Physical and chemical stability studies indicated that the optimally formulated CDD-loaded chitosan/alginate nanoparticles were stable at 4 °C for 3 months.

1. Introduction

Nanotechnology is an emerging technology that can be used in a broad range of research areas, including material, medical and pharmaceutical sciences (Ali and Sinha 2014). The major focus of nanotechnology research in the pharmaceutical sciences is the design of more selective and effective nanoparticles that can be used as carriers of bioactive compounds for enteral and parenteral administration, with protection of these compounds from enzymatic degradation, metabolism and cellular efflux and extension of shelf-life (Motwani et al. 2008), Nanoparticles can also be used to deliver bioactive compounds to their target at the appropriate time and dosage (Sekhon 2010).

Bioactive compounds extracted from plants have become alternatives for treatment of various diseases due to their low toxicity and lack of side effects (Ukil et al. 2003). Curcumin, the major component of turmeric (*Curcuma longa* L.), has been extensively used as a flavor, coloring in food, preservative and household medicine in Southern Asia for a century. Curcumin has pharmacological effects including anti-oxidant, anti-inflammatory, anti-tumor, anti-HIV and anti-infectious activities (Ukil et al. 2003; Cousins et al. 2007). However, curcumin also has limitations due to its low water solubility, low stability, poor bioavailability and rapid intestinal and hepatic degradation and metabolism (Anand et al. 2007; Yang et al. 2012). Therefore, several approaches have been made to overcome these limitations, including development of nanoparticle formulations of curcumin (Bisht et al. 2007) and chemical conjugation to give curcumin prodrugs (Wichitnithad et al. 2011).

Curcumin diethyl disuccinate (CDD) (Fig. 1) is a succinate prodrug of curcuminoids that is synthesized by aldol condensation of 2,4-pentanedione with benzaldehyde and esterification with the methyl or ethyl ester of succinyl chloride. Compared to other succinate prodrugs of curcuminoids and to curcumin itself, CDD has better stability in human plasma and improved anti-colon cancer activity (Wichitnithad et al. 2011). These properties may be further improved by encapsulation of CDD in nanoparticles.

Nanoparticles can be formulated from synthetic biodegradable polymers, lipids, proteins, and polysaccharides (Ghalandarlaki et al. 2014). Alginate and chitosan are polysaccharides that have been extensively used for controlled release and delivery of bioactive compounds to target sites (Lertsutthiwong and Rojsitthisak 2011; Azevedo et al. 2014; Bhunchu and Rojsitthisak 2014).

Alginate is a hydrophilic polysaccharide extracted from marine brown algae. It is a linear copolymer of β-D-mannuronic acid and α-L-guluronic acid linked by 1,4-glycosidic bonds (Lertsutthiwong et al. 2009). Alginate is of interest in pharmaceutical applications due to its gel formation ability, biocompatibility, non-toxicity, biodegradability and mucoadhesiveness (Lertsutthiwong et al. 2010). Alginate nanoparticles can be obtained by inducing gelation with divalent cations (Lertsutthiwong et al. 2008; Li et al. 2008). This simple gelling property allows alginate to be used to produce a pre-gel consisting of very small aggregates of particles, followed by addition of an aqueous polycationic solution to make a polyelectrolyte complex (Lertsutthiwong et al. 2009). For example, poly-L-lysine (PLL), a cationic natural polymer, has been used in combination with alginate to prepare nanoparticles (De and Robinson 2003). However, PLL is toxic and immunogenic for administration by injection, and chitosan can be used as an alternative cationic polymer (De and Robinson 2003).

Chitosan is a linear polysaccharide consisting of D-glucosamine and *N*-acetyl-D-glucosamine units linked by β(1→4) glycosidic linkages. Chitosan has versatile properties of biodegradability, biocompatibility, mucoadhesiveness, non-toxicity and good film formation (Bhunchu and Rojsitthisak 2014). For example, leakage of drugs from alginate nanoparticles is reduced when chitosan is used as a secondary counterion source (Zhang et al. 2011). Chitosan can enhance the desirable properties of alginate particles, such as controlled release, permeability, stability and half-life in physiological fluids (Zhang et al. 2011). Our previous work (Bhunchu et al., unpublished data) demonstrated that the use of lower molecular

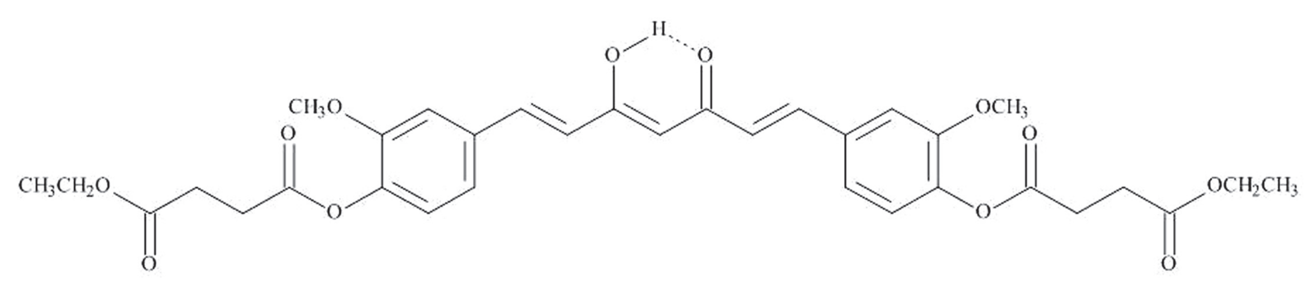

Fig. 1: Structure of curcumin diethyl disuccinate

Table 1: Factors and levels in Box-Behnken design

Factors	Level used, Actual (coded)		
	Low (-1)	Medium (0)	High (+1)
X_1 = Chitosan/alginate mass ratio	0.05:1	0.10:1	0.15:1
X_2 = Pluronic F127 (%w/v)	0.5	1	1.5
X_3 = CDD (mg/ml)	0.5	1	1.5
Responses:	Constraints		
Y_1 = Particle size (nm)	Minimize		
Y_2 = Zeta potential (mV)	$Y_2 \geq 20$		
Y_3 = Encapsulation efficiency (%)	Maximize		
Y_4 = Loading capacity (%)	Maximize		

the optimized CDD-loaded nanoparticles in MDA-MB-231 breast cancer cells were investigated.

2. Investigations, results and discussion

2.1. Formation of CDD-loaded chitosan/alginate nanoparticles

Preparation of CDD-loaded chitosan/alginate nanoparticles by o/w emulsification and ionotropic gelation under mild conditions at room temperature was simple, rapid and reliable. The CDD encapsulation efficiency (~17-45%) and loading capacity (~1-5%) of the nanoparticles were low due to the hydrophilic and hydrophobic characters of the nanoparticle matrices and CDD, respectively. Li et al. (2008)

Table 2: Factors and observed responses in Box-Behnken design (n = 3)

Runs	Factors			Responses			
	X_1	X_2 (%w/v)	X_3 (mg/ml)	Y_1 (nm)	Y_2 (mV)	Y_3 (%)	Y_4 (%)
1	0.05	0.50	1.00	279 ± 71	-27.8 ± 0.3	38.71 ± 2.78	3.43 ± 0.34
2	0.15	0.50	1.00	434 ± 17	-19.8 ± 1.4	17.08 ± 2.27	1.41 ± 0.21
3	0.05	1.50	1.00	308 ± 22	-17.5 ± 0.2	25.42 ± 1.12	2.14 ± 0.04
4	0.15	1.50	1.00	645 ± 24	-12.4 ± 0.5	13.64 ± 0.87	1.06 ± 0.11
5	0.05	1.00	0.50	285 ± 22	-24.9 ± 1.3	24.52 ± 1.91	1.25 ± 0.12
6	0.15	1.00	0.50	558 ± 16	-16.5 ± 1.2	19.09 ± 4.32	0.76 ± 0.16
7	0.05	1.00	1.50	340 ± 33	-23.2 ± 0.1	39.97 ± 2.37	4.45 ± 0.35
8	0.15	1.00	1.50	585 ± 16	-17.1 ± 0.3	16.55 ± 1.82	2.83 ± 0.25
9	0.10	0.50	0.50	427 ± 26	-25.7 ± 0.5	35.16 ± 0.96	1.16 ± 0.08
10	0.10	1.50	0.50	615 ± 29	-13.4 ± 0.8	23.38 ± 1.43	2.48 ± 0.13
11	0.10	0.50	1.50	482 ± 15	-20.8 ± 0.5	40.12 ± 3.04	5.25 ± 0.28
12	0.10	1.50	1.50	607 ± 27	-17.2 ± 1.2	37.37 ± 3.29	3.21 ± 0.24
13[a]	0.10	1.00	1.00	505 ± 19	-21.0 ± 0.7	45.11 ± 1.43	3.78 ± 0.12
14[a]	0.10	1.00	1.00	529 ± 7	-20.6 ± 0.4	43.44 ± 1.31	3.51 ± 0.05
15[a]	0.10	1.00	1.00	519 ± 14	-22.3 ± 0.5	44.31 ± 1.03	3.57 ± 0.11

[a] indicates the center point of the design.

weight chitosan produced smaller chitosan/alginate nanoparticles with higher encapsulation and loading capacity of CDD at an optimal $CaCl_2$/alginate mass ratio of 0.2:1. In addition, chitosan/alginate nanoparticles improved uptake of CDD in caco-2 cells (Bhunchu et al. 2015). However, a systematic study of the optimal formulation of CDD-loaded chitosan/alginate nanoparticles is required. Therefore, in the current study, Box-Behnken statistical design was used to design and optimize CDD-loaded chitosan/alginate nanoparticles using response surface methodology. The influence of the chitosan/alginate mass ratio and concentrations of Pluronic F127 and CDD on the characteristics of the nanoparticles was examined, and the *in vitro* cytotoxicity and cellular uptake of also concluded that use of hydrophilic polymeric nanoparticles for encapsulation of hydrophobic compounds is difficult and that the encapsulation mechanism is unclear. Therefore, the challenge of this study was to maximize the encapsulation efficiency and loading capacity using chitosan/alginate nanoparticles by optimization of the preparation process using statistical design.

Previous work showed that Pluronic F127 should be used as a stabilizer in the preparation process because Pluronic F127 contains high hydrophilicity-lipophilicity balance value which makes it more soluble in water and enhance the solubility of CDD. In addition, 1% (w/v) Pluronic F127 gave the smallest particles with the highest encapsulation efficiency and loading capacity,

Table 3: Summary of results of regression analysis responses

Model	F-value	SD	R^2	Adjusted-R^2	Predicted-R^2	PRESS	CV (%)	Remark
Particle size (Y_1)								
Linear	36.39	65.99	0.7803	0.7203	0.5594	65.99	13.98	-
Interaction (2FI)	6.44	68.38	0.8284	0.6997	0.2119	68.38	14.49	-
Quadratic	74.76	17.93	0.9926	0.9793	0.9003	17.93	3.80	Suggested
Zeta potential (Y_2)								
Linear	25.39	1.77	0.8738	0.8394	0.7544	66.78	1.77	-
Interaction (2FI)	29.26	1.22	0.9564	0.9237	0.8717	34.89	1.22	-
Quadratic	67.67	0.67	0.9919	0.9772	0.9469	14.43	0.67	Suggested
Encapsulation efficiency (Y_3)								
Linear	2.62	9.79	0.4166	0.2575	0.0435	1728.34	9.79	-
Interaction (2FI)	1.26	10.77	0.4865	0.1013	0.5033	2716.39	10.77	-
Quadratic	80.29	1.58	0.9931	0.9808	0.9256	134.50	1.58	Suggested
Loading capacity (Y_4)								
Linear	6.73	0.92	0.6474	0.5512	0.3498	17.06	0.92	-
Interaction (2FI)	4.59	0.86	0.7749	0.6061	0.2429	19.87	0.86	-
Quadratic	68.33	0.21	0.9919	0.9774	0.8954	2.74	0.21	Suggested

Remark: Only significant terms are included.

Table 4: Summary of lack of fit and adequate precision for each response

Model	Sum of square	Lack of fit F-value	p-value Prob > F	Adequacy precision	Remark
Particle size (Y_1)					
Linear model	47604.52	36.39	0.0270	11.467	-
Interaction model (2FI)	37116.02	42.56	0.0231	8.507	-
Quadratic model	1317.25	3.02	0.2585	26.687	Suggestion
Zeta potential (Y_2)					
Linear model	32.79	4.77	0.0852	16.802	-
Interaction model (2FI)	10.32	2.25	0.0388	18.433	-
Quadratic model	0.69	0.30	0.8270	28.205	Suggestion
Encapsulation efficiency (Y_3)					
Linear model	1049.52	49.98	0.0198	4.698	-
Interaction model (2FI)	923.27	65.95	0.0150	3.653	-
Quadratic model	7.75	1.11	0.5069	23.089	Suggestion
Loading capacity (Y_4)					
Linear model	9.21	43.84	0.0225	8.128	-
Interaction model (2FI)	5.86	41.86	0.0235	7.070	-
Quadratic model	0.16	2.36	0.3117	27.977	Suggestion

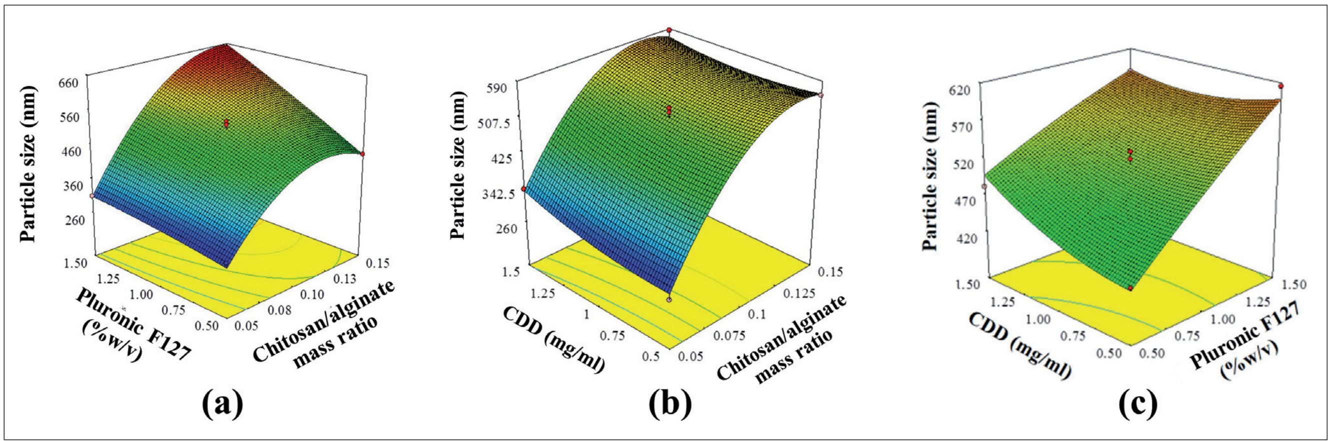

Fig. 2: Three dimensional response surface plots showing the effect on particle size (Y_1) of (a) chitosan/alginate mass ratio (X_1) and Pluronic F127 concentration (X_2); (b) chitosan/alginate mass ratio (X_1) and CDD concentration (X_3); (c) Pluronic F127 concentration (X_2) and CDD concentration (X_3).

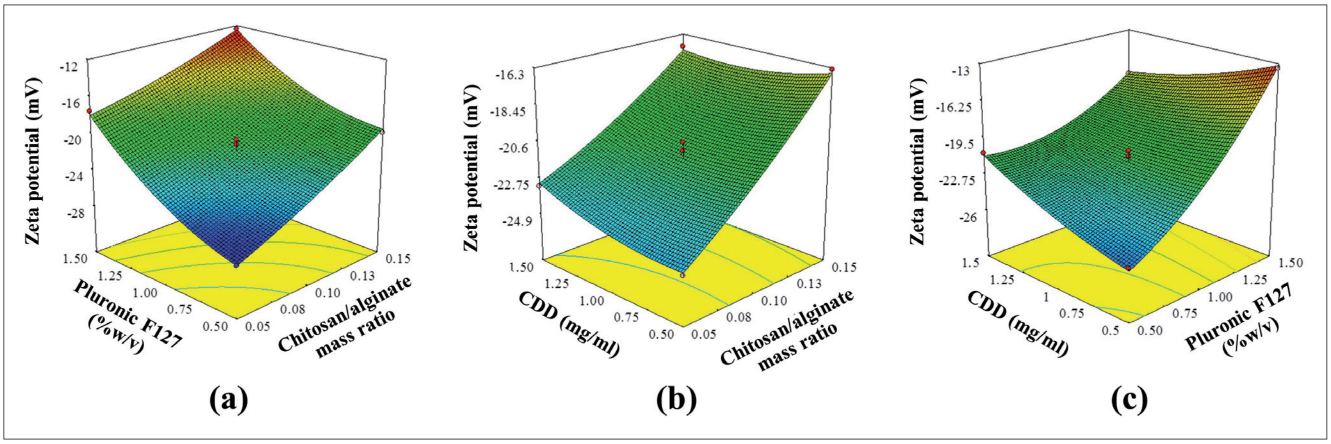

Fig. 3: Three dimensional response surface plots showing the effect on zeta potential of (a) chitosan/alginate mass ratio (X_1) and Pluronic F127 (X_2); (b) chitosan/alginate mass ratio (X_1) and CDD (X_3); (c) Pluronic F127 (X_2) and CDD (X_3).

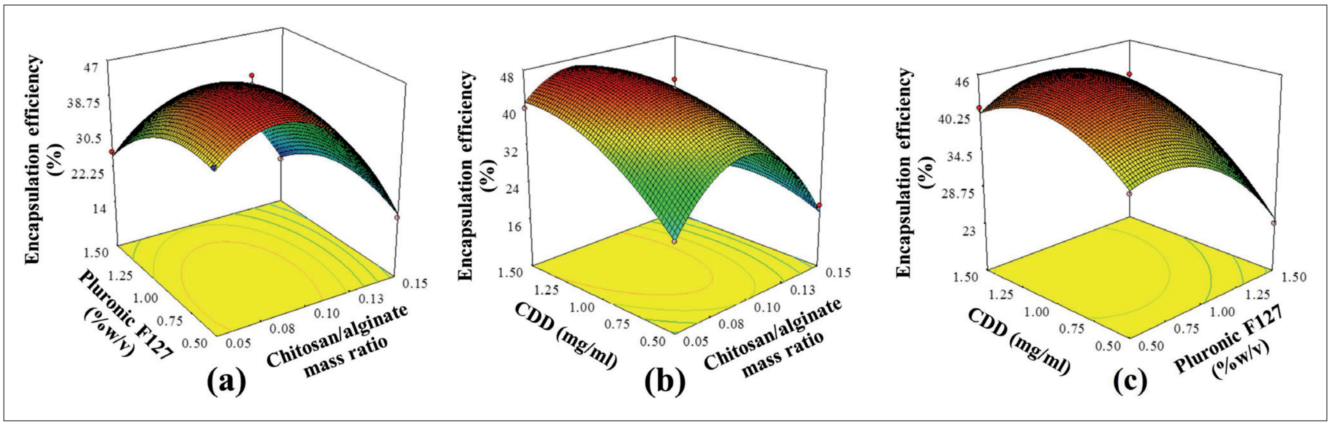

Fig. 4: Three dimensional response surface plots showing the effect on encapsulation efficiency of (a) chitosan/alginate mass ratio (X_1) and Pluronic F127 (X_2); (b) chitosan/alginate mass ratio (X_1) and CDD concentration (X_3); (c) Pluronic F127 concentration (X_2) and CDD concentration (X_3).

compared to Tween 80® and Cremophor[RH] (Bhunchu et al. 2015). Therefore Pluronic F127 was chosen for this study, with Box-Behnken design and RSM used for optimization of the formulation (Table 1). Chitosan/alginate mass ratio and Pluronic F127 and CDD concentrations were used as the main factors affecting the characteristics (responses) of the nanoparticles, and the most important responses were particle size, zeta potential, encapsulation efficiency and loading capacity. Chitosan/alginate mass ratios of 0.05:1 to 0.15:1 were examined because below this lower mass ratio resulted in the reduction of encapsulation efficiency, whereas beyond 0.15:1 the particles aggregate and form microparticles. For Pluronic F127, <0.5% (w/v) is insufficient to stabilize the CDD-loaded nanoparticle suspension and >1.5% (w/v) produces a viscous system due to particle aggregation. The solubility of CDD in acetone is 1.5 mg/ml, and therefore CDD concentrations of 0.05 to 1.5 mg/ml were examined. Thus, the 15 experiments in Table 1 were performed using a three-factor, three-level design.

The results (Table 2) showed that the particle size mainly depended on the chitosan/alginate mass ratio and Pluronic F127 concentration. The minimum size of 279 nm occurred at a chitosan/alginate mass ratio of 0.05:1 and 0.5% (w/v) Pluronic F127 (formulation 1), and the maximum size of 645 nm corresponded to the highest chitosan/alginate mass ratio (0.15:1) and highest Pluronic F127 concentration (1.5% w/v) (formulation 4). The zeta potential was mainly affected by the chitosan/alginate mass ratio and became less negative with a higher mass ratio at fixed Pluronic F127 and CDD concentrations. For example, at 0.50% (w/v) Pluronic F127 and 1 mg/ml CDD, the zeta potential changed from -27.8 to -19.8 mV when the chitosan/alginate mass ratio increased from 0.05:1 to 0.15:1 (formulation 1 vs. 2). This could be explained by the charge density of chitosan. A higher chitosan/alginate ratio results in more cations in the system that can neutralize anions on alginate during nanoparticle formation, which produces a less negative zeta potential. The highest encapsulation efficiency of the nanoparticles was observed at a chitosan/alginate mass ratio of 0.1:1, 1% (w/v) Pluronic F127and 1 mg/ml CDD (formulations 13-15), and the highest loading capacity of about 5% occurred at a 0.1:1 chitosan/alginate mass ratio, 0.5% (w/v) Pluronic F127 and 1.5 mg/ml CDD (formulation 11).

2.2. *Fitting data to model*

Responses for all 15 formulations were simultaneously fitted to linear, interaction (2FI) and quadratic models using Design Expert® software. To evaluate the effect of formulation parameters on each response (Y_1-Y_4), a polynomial equation with ANOVA was used. The comparative values of R^2, adjusted R^2, predicted R^2, SD, CV and PRESS are shown in Table 3. Responses Y_1-Y_4 best followed a quadratic model based on the high values of R^2, adjusted R^2 and predicted R^2 and the low values of SD, PRESS and CV. Only significant ($p<0.05$) coefficients are included in the polynomial equations. PRESS is a particularly important measure of fit of the model to the points in the design. The smaller the PRESS statistic, the better the model fits to the data points (Segurola et al. 1999).

2.3. *Response surface analysis by polynomial equation*

Response surfaces analyzed by polynomial equation are useful for determination of the interaction effects of two factors on the responses while the third factor is kept constant (Woitiski et al. 2009). In the polynomial equation, a positive value indicates a

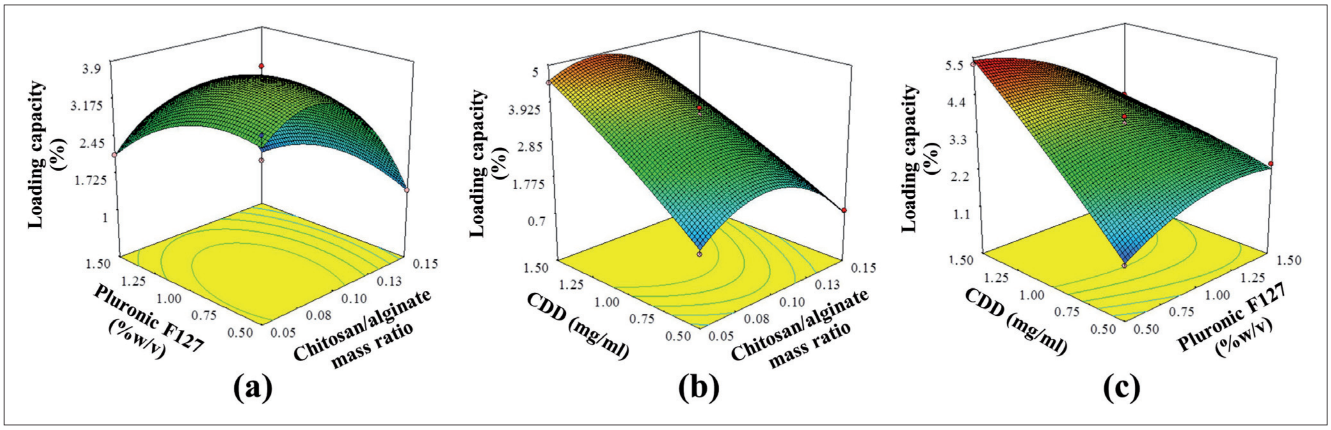

Fig. 5: Three dimensional response surface plots showing the effect on loading capacity of (a) chitosan/alginate mass ratio (X_1) and Pluronic F127 concentration (X_2); (b) chitosan/alginate mass ratio (X_1) and CDD concentration (X_3); (c) Pluronic F127 concentration (X_2) and CDD concentration (X_3).

Table 5: Optimal formulation, observed and predicted values for the responses, and the % error

Optimized formulation composition (X_1; X_2; X_3)	Response variable	Observed value	Predicted value	% error[a]
0.05:1; 0.65 % (w/v); 1.5 (mg/ml)	Y_1 (nm)	324 ± 29	335.78	- 3.51
	Y_2 (mV)	-25.24 ± 1.3	-24.16	+4.47
	Y_3 (%)	44.24 ± 3.4	41.91	+5.56
	Y_4 (%)	5.56 ± 0.2	5.32	+4.51

[a] % error = (observed value - predicted value)/predicted value × 100

synergistic effect through which the response increases proportional to the factor. In contrast, a negative value indicates an inverse relationship (antagonistic effect) between the response and factors. The criteria for selection of the suitable model are highest *F*-value and adequate precision, but lowest lack of fit *F*-value, and the adjusted R^2 and predicted R^2 should be close to 1 (Tables 3 and 4). The best quadratic model for particle size, zeta potential, encapsulation efficiency and loading capacity was as follows:

is most appropriate for zeta potential (Tables 3 and 4). The response surface plots in Fig. 3 show that the chitosan/alginate mass ratio had the main influence on zeta potential. Increasing the chitosan/alginate mass ratio caused increasingly less negative zeta potential of the CDD-loaded nanoparticles. De and Robinson (2003) suggested that a higher percentage of chitosan increased the chance of neutralization of amino groups of chitosan with carboxylate groups of alginate, and consequently increased the zeta potential (less negative). Similar results were observed by Arora et al. (2011) and Araujo et al. (2013).

The encapsulation efficiency of the CDD-loaded nanoparticles ranged from 13.64% (formulation 4) to 45.11% (formulation 13). The relatively low encapsulation efficiency is due to the hydrophilic nature of the chitosan/alginate nanoparticles, which makes it relatively difficult to encapsulate hydrophobic CDD; and because the hydrophobic nature of CDD results in a larger loss of CDD to the external aqueous phase during formulation. The low encapsulation efficiency is in agreement with the study of Li et al. (2008), in which the low encapsulation of hydrophobic molecules in chitosan/alginate nanoparticles was suggested to be due to their incompatibility with the hydrophilic polymers.

$$Y_1 = 517.67 + 128.62X_1 + 66.75X_2 + 16.13X_3 + 45.25X_1X_2 - 12X_1X_3 - 20.75X_2X_3 - 95.83X_1^2 - 5.08X_2^2 + 15.17X_3^2 \quad (1)$$

$$Y_2 = -21.33 + 4.2X_1 + 3.46X_2 + 1.26X_3 - 0.73X_1X_2 - 0.6X_1X_3 - 2.17X_2X_3 + 0.42X_1^2 + 1.54X_2^2 + 0.52X_3^2 \quad (2)$$

$$Y_3 = 44.33 - 7.75X_1 - 4.13X_2 + 4.13X_3 + 2.5X_1X_2 - 4.5X_1X_3 - 2.25X_2X_3 - 14.79X_1^2 - 5.54X_2^2 - 4.54X_3^2 \quad (3)$$

$$Y_4 = 3.63 - 0.68X_1 - 033X_2 + 1.25X_3 + 023X_1X_2 - 0.33X_1X_3 - 0.82X_2X_3 - 1.18X_1^2 - 0.48X_2^2 - 0.13X_3^2 \quad (4)$$

According to Eq. (1), X_1, X_2, X_1X_2 and X_1^2 were significant ($p<0.05$). The effects are presented as 3-dimensional response surface plots in Fig. 2. The chitosan/alginate mass ratio (Fig. 2 a) and Pluronic F127 concentration (Fig. 2 c) both had positive effects on particle size, whereas the CDD concentration did not have a significant effect (Fig. 2 b, 2 c). ANOVA also indicated that the particle size strongly depended on the chitosan/alginate mass ratio and Pluronic F127. Therefore, low levels for these two factors were favorable for preparation of CDD-loaded nanoparticles. This might be due to Pluronic F127 forming micelles surrounding the hydrophobic CDD with its hydrophilic groups facing the alginate polymer network. An increase in the Pluronic F127 concentration increased the chance of interaction with alginate, resulting in a larger particle size. Addition of chitosan to the alginate nanoparticle suspension led to formation of chitosan network on the surface of the alginate nanoparticles, again resulting in a larger particle size. To avoid aggregation of large particles, Pluronic F127 should not be higher than 1% (w/v) (Kim et al. 2013).

In Eq. (2), all three factors of chitosan/alginate mass ratio (*X1*), Pluronic F127 (*X2*) and CDD (*X3*) concentrations have synergistic effects on the zeta potential. To select a suitable model, *F*-value and R^2 should be high, but the lack of fit *F*-value should be low. Therefore, the quadratic model

In Eq. (3), the negative values for X_1 and X_2 represent an antagonistic effect while the positive value of X_3 indicates a synergistic effect. Response surface plots for encapsulation efficiency as a function of chitosan/alginate mass ratio, Pluronic F127 and CDD concentrations are shown in Fig. 4. The encapsulation efficiency depended on all three factors. The value increased as the chitosan/alginate mass ratio increased to 0.10:1, regardless of the Pluronic F127 and CDD concentrations. This might be because the chitosan layer coated on the surface of alginate nanoparticles reduces leakage of CDD from the nanoparticles to the aqueous phase. Sarmento et al. (2007) also found that the encapsulation efficiency of chitosan/alginate nanoparticles increased with an increase in chitosan/alginate mass ratio due to the compact structure of the nanoparticle matrix. However, a further increase in the chitosan/alginate mass ratio to 0.15:1 resulted in lower encapsulation efficiency. An increase in Pluronic F127 up to 1% (w/v) led to an increase in the solubility of the CDD in the aqueous phase by self-assembly in the aqueous environment. The CDD was localized in the hydrophobic core of Pluronic F127, while the hydrophilic parts of Pluronic F127 faced hydrophilic polymers in the aqueous phase. However, the encapsulation efficiency of the CDD-loaded nanoparticles decreased with a further increase of Pluronic F127

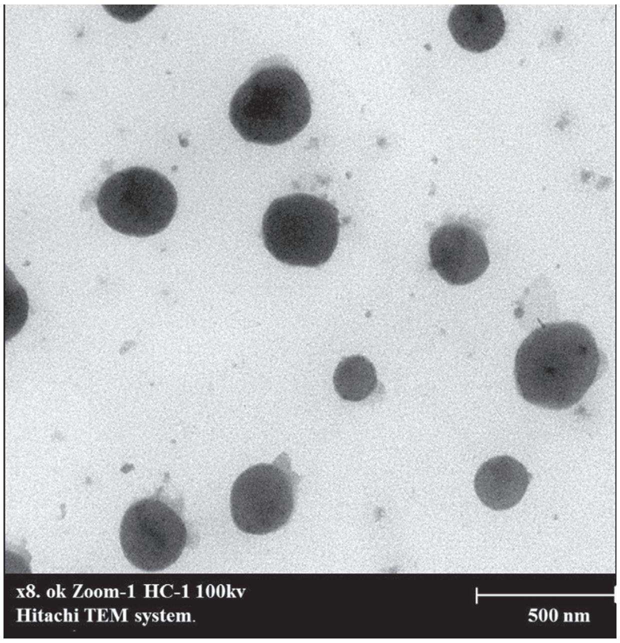

Fig. 6: TEM image of CDD-loaded nanoparticles.

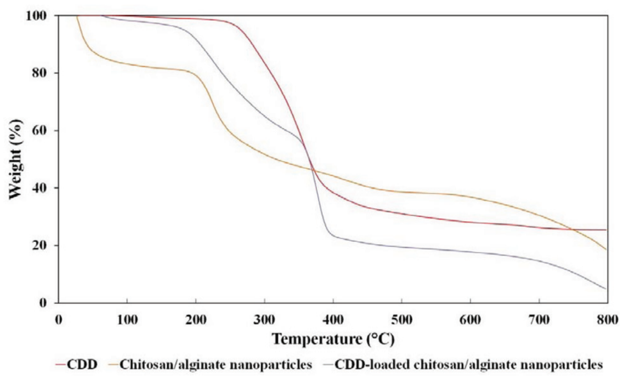

Fig. 7: Thermal gravimetric curves for CDD and chitosan/alginate and CDD-loaded nanoparticles.

(1.5%, w/v). The encapsulation efficiency was consistently increased by increasing the CDD concentration.

The loading capacity of the CDD-loaded nanoparticles ranged from 1.06% (formulation 4) to 5.25% (formulation 11). In Eq. (4), the negative values of X_1 and X_2 indicate an inverse relationship and the positive value of X_3 indicates a favorable effect of an increase on the loading capacity. That is, an increase in the CDD concentration had a synergistic effect on the loading capacity and caused an increase in loading capacity (Fig. 5 b and Fig. 5 c). Increases of the chitosan/alginate mass ratio and Pluronic F127 concentrations from low to intermediate levels also resulted in an increase in loading capacity. This might be due to having a sufficient quantity of polymers for encapsulation of CDD. However, high levels of both factors resulted in lower loading capacity.

2.4. *Optimization and validation of the model*

Process optimization was performed with a desirability function (δ) to optimize the four responses simultaneously using Design Expert® software. A high value of the desirability coefficient ($0 \leq \delta \leq 1$) indicates that the operating point can produce acceptable formulation results (Ranjan et al. 2012). The optimal formulation

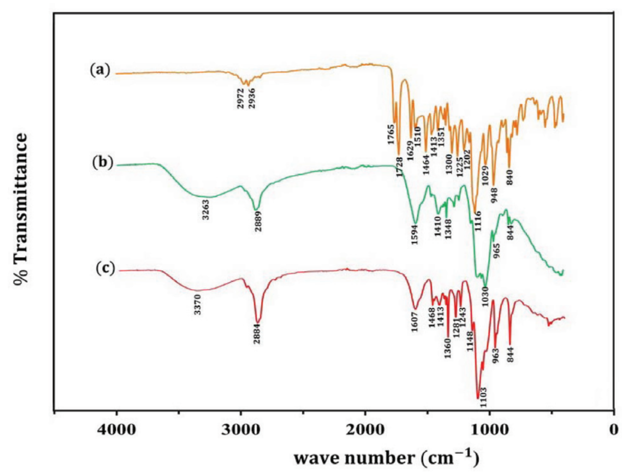

Fig. 8: FT-IR spectra of (a) CDD powder, (b) chitosan/alginate nanoparticles and (c) CDD-loaded chitosan/alginate nanoparticles.

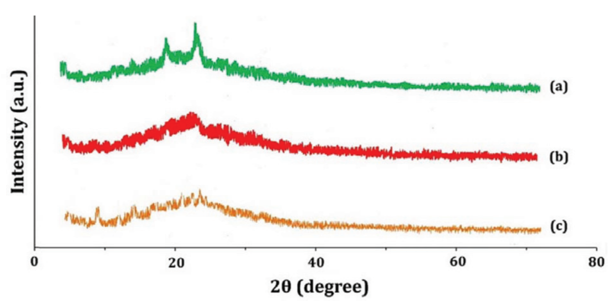

Fig. 9: XRD patterns of (a) CDD powder, (b) chitosan/alginate nanoparticles and (c) CDD-loaded chitosan/alginate nanoparticles.

was selected based on the criteria of minimum particle size, zeta potential in the range of -30 to -20 mV, and maximum encapsulation efficiency and loading capacity. The maximum value of the desirability coefficient was obtained at a formulation with a chitosan/alginate mass ratio of 0.05:1, 0.65% (w/v) Pluronic F127, and 1.5 mg/ml CDD, and this formulation fulfilled the requirements for the optimal formulation. To validate this optimal formulation, CDD-loaded nanoparticles were prepared using the optimized conditions and the observed values of the responses were compared with the predicted values. The results in Table 5 show that the observed and predicted values of the responses were acceptable because of the % error, which showed adequate precision for the prediction of the optimized condition.

2.5. *Characterization of the optimized formulation*

CDD-loaded chitosan/alginate nanoparticles produced from the optimal formulation (chitosan/alginate mass ratio of 0.05:1, 0.65% (w/v) Pluronic F127 and 1.5 mg/ml CDD) were visualized using TEM (Fig. 6). The TEM image confirmed that the CDD-loaded nanoparticles had a well-defined spherical shape and a solid dense structure.

Thermal gravimetric analysis (TGA) (Fig. 7) showed that CDD powder decomposed at 280-400 °C, resulting in 60% weight loss. In chitosan/alginate nanoparticles (without CDD), initial weight loss occurred at 25-150 °C due to evaporation of moisture in the nanoparticles (Fig. 7). A second weight loss (~47%) occurred at 200-500 °C. After encapsulation of CDD in chitosan/alginate nanoparticles, the second weight loss (~40%) occurred at the same temperature as that for the empty nanoparticles, With increasing temperature, the weight of both blank and drug loaded-nanopar-

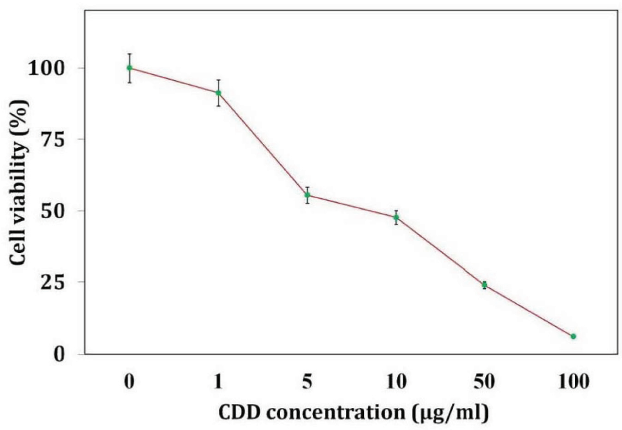

(a)

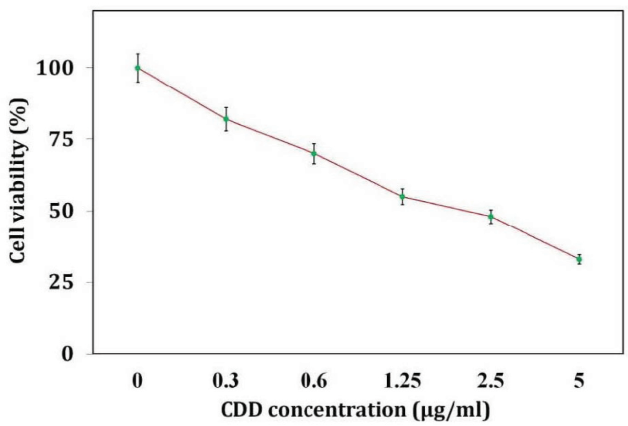

(b)

Fig. 10: Survival of MDA-MB-231 cell lines in a MTT assay after treatment with (a) free CDD and (b) CDD-loaded nanoparticles for 72 h.

Table 6: IC_{50} values for free CDD and CDD-loaded nanoparticles in MDA-MB-231 cells

Sample	IC_{50} (μg/ml)
Free CDD	9
CDD-loaded nanoparticles	2

ticles decreased slowly from 45-190 °C due to moisture evaporation (Paula et al. 2010), then decreased rapidly from 190-350 °C, and then slowly again at higher temperature, possibly due to loss of small molecules and breaking of crosslinking and thermal degradation of the ionic complex between chitosan and alginate in the polymer matrix (Gomathi et al. 2014). However, the weight of CDD-loaded nanoparticles then rapidly decreased again at 350-400 °C, resulting in around 70% weight loss. This occurred in the same thermal decomposition range observed for CDD alone, and this weight-loss pattern did not occur for the chitosan/alginate nanoparticles. These results indicate that CDD was encapsulated into nanoparticles. The thermal decomposition of CDD began at 280 °C, while the CDD-loaded nanoparticles shows delayed onset of the degradation, shifting to higher temperature of 350 °C which suggests that the thermal stability of CDD is enhanced by encapsulation. After thermal decomposition, 25.45% of CDD, 22.24% of chitosan/alginate nanoparticles and 5.15% of CDD-loaded chitosan/alginate nanoparticles remained, indicating high thermal stabilities and confirming the reported slow degradation rate (Gomathi et al. 2014).

The encapsulation of CDD suggested in TGA was confirmed by FT-IR (Fig. 8) and X-ray diffraction (Fig. 9). In FT-IR spectra of CDD, blank nanoparticles and CDD-loaded nanoparticles, characteristic peaks for CDD were observed at 2972-2936, 1765, 1728, 1510 and 1464 cm^{-1}. These peaks were also present in the FT-IR spectrum of CDD-loaded nanoparticles with some broadening and reduction intensity, indicating the absence of chemical interactions between CDD and polymers after nanoparticles formulation. However, disappearance of the bands at 1765 and 1728 cm^{-1}, which are represented the C = O stretching of the aliphatic and phenolic esters (Sun et al. 2013), respectively, were observed in CDD-loaded nanoparticles. Micelle formation in nanoparticles may have resulted in loss of these signals. The additional bands in the spectrum of the CDD-loaded nanoparticles (i.e. 3370, 2884 and 1360 cm^{-1}) are due to OH stretching in alginate and chitosan, and C-H bending and C-H stretching in Pluronic F127, respectively (Sugama and Cook 2000; Sankalia et al. 2007; Yang et al. 2013). The characteristic peaks of CDD in the spectrum of the CDD-loaded nanoparticles suggest that CDD was encapsulated in the chitosan/alginate nanoparticles at the molecular level and that micelle formation in the nanoparticle preparation did not cause breakdown of the CDD structure (Kharia et al. 2012).

In X-ray diffraction analysis of CDD powder, chitosan/alginate nanoparticles and CDD-loaded nanoparticles, the peaks for CDD at 18.6 Å and 23.4 Å were merged and had reduced intensity after encapsulation in the chitosan/alginate nanoparticles, indicating that CDD was encapsulated in the amorphous state.

2.6. *In vitro cytotoxicity*

According to previous work (Rojsitthisak et al., unpublished data), both free CDD and CDD-loaded nanoparticles produced from optimal condition did not show significantly cytotoxic effect on MDA-MB-231 cells at 24 h and 48 h, whereas they affected on the cancer cells at 72 h. Therefore, the cytotoxicity assay in this study was carried out at 72 h. In addition, blank chitosan/alginate nanoparticles (without CDD) showed no cytotoxic effect to cancer cells for the longest duration of exposure time (72 h). It might be suggested that the blank chitosan/alginate nanoparticles prepared by the condition as described in the methodology were not caused cytotoxic effect on MDA-MB-231 cells.

Viability of cells after culturing with free CDD and CDD-loaded nanoparticles for 72 h is shown in Fig. 10. Both free CDD and CDD-loaded nanoparticles decreased the cancer cell viability, but the CDD-loaded nanoparticles have a stronger effect than free CDD. For example, the viability of MDA-MB-231 cells after treatment with free CDD at 5 μg/ml was about 55%, whereas that of CDD-loaded nanoparticles was about 33%.

The IC_{50} of free CDD and CDD-loaded nanoparticles were about 9 and 2 μg/ml, respectively, indicating that both free CDD and CDD-loaded nanoparticles were toxic to these cells. The cytotoxicity of CDD-loaded nanoparticles increased significantly ($p<0.05$) with increasing CDD concentration. The greater toxicity of the CDD-loaded nanoparticles might be due to enhanced cellular uptake, as examined in the following section.

2.7. *In vitro cellular uptake*

To confirm the cytotoxic effect of CDD-loaded nanoparticles on the MDA-MB-231 cells, the cellular uptake assay was then performed at similar exposure time with cytotoxicity assay. The results shows that the cellular uptake of free CDD and CDD-loaded nanoparticles by MDA-MB-231 cells after incubation for 72 h was visualized using a confocal laser scanning microscope (Fig. 11). Since the chemical structure of CDD contains a fluorophore with the maximum excitation and emission wavelengths of 400 and 470 nm, respectively, the fluorescent dye is not required. The fluorescence intensity was markedly higher in cells treated with CDD-loaded nanoparticles compared with those treated with free CDD, and

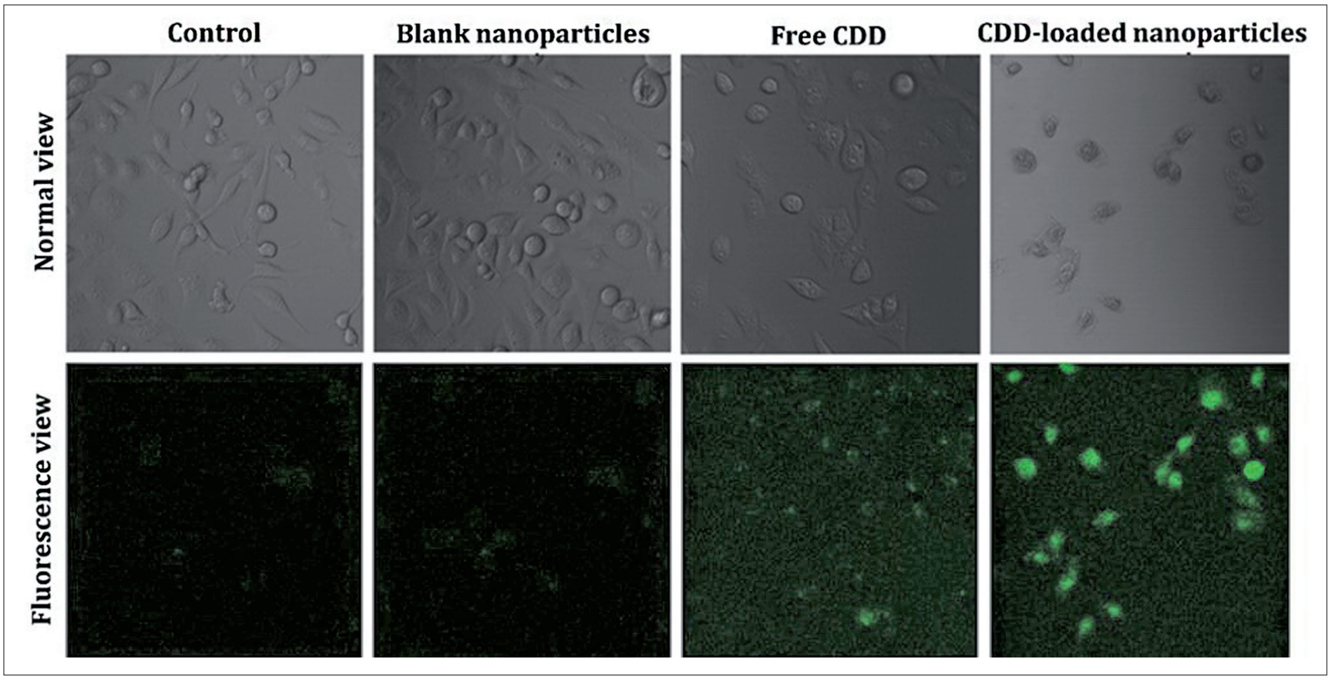

Fig. 11: Confocal laser scanning microscopy images of MDA-MB-231 cells after incubation with blank nanoparticles, free CDD and CDD-loaded nanoparticles at 37 °C for 72 h.

Table 7: Stability of the optimal formulation of CDD-loaded nanoparticles at 25 ºC and 4 ºC (n = 3)

Storage condition	Time (months)	Particle size (nm)	Zeta potential (mV)	Encapsulation efficiency (%)
4 ºC	0	328 35	-26.5 1.3	42.7 3.3
	1	336 19	-27.9 1.1	41.3 0.2
	2	388 33	-24.2 0.5	39.8 3.2
	3	412 29	-22.3 0.8	36.3 1.4
25 ºC	0	328 35	-26.5 1.3	42.7 3.3
	1	378 47	-24.1 0.7	40.1 0.6
	2	436 28	-20.5 2.1	32.4 2.1
	3	765 39	-15.9 1.9	19.9 1.8

there was no observable fluorescence in cells incubated with blank nanoparticles. This indicates that CDD-loaded nanoparticles were taken up by MDA-MB-231 breast cancer cells more effectively than free CDD, resulting in improved cytotoxicity (Table 6). Many studies demonstrated that the cellular uptake of nanoparticles depended on size and surface charges of nanoparticles (Bhunchu et al. 2015; Chuah et al. 2014; Kunwar et al. 2008). Bhunchu et al. (2015) found similar results in Caco-2 cells and concluded that chitosan-alginate nanoparticles can improve cellular uptake and delivery of CDD into Caco-2 cells. The improved uptake and prolonged duration of CDD nanoparticles in cells of up to 72 h are consistent with previous findings for nanoformulation containing hydrophobic molecules such as curcumin (Kunwar et al. 2008; Chuah et al. 2014).

2.8. Stability

The stability of nanoparticles produced from the optimal formulation was determined at 4 °C and 25 °C for 3 months (Table 7). At 4 °C, the particle size slightly increased and the negative value of the zeta potential and encapsulation efficiency slightly decreased. However, the zeta potential remained in the range of -20 to -30 mV, which indicates good stability of the particle suspension in aqueous medium (Bhunchu et al. 2015). At 25 °C, the particle size sharply increased due to aggregation and consequently the negative value of zeta potential and encapsulation efficiency decreased significantly compared to of the changes at 4 °C. For example, the encapsulation efficiency after storage at 25 °C for 3 months was decreased by about 53%, compared to a decrease of 15% at 4 °C. This might be explained that the degradation of polymer matrices in the suspension at 25 °C was faster than that at 4 °C and caused more drug leakage (Abdelwahed et al. 2006). Therefore, storage of the nanoparticles at 4 °C is required to reduce the risk of particle aggregation and CDD leakage.

General conclusion, response surface statistical modeling using Box-Behnken design was successfully applied in development of chitosan/alginate nanoparticles for CDD delivery. Variables of chitosan/alginate mass ratio and Pluronic F127 and CDD concentrations influenced the particle size, zeta potential, encapsulation efficiency and loading capacity of the nanoparticles. The optimized formulation prepared using the predicted levels for these variables had a particle size of 324 nm, zeta potential of -25.2 mV, encapsulation efficiency of 44.2% and loading capacity of 5.6%. These chitosan-alginate nanoparticles enhanced the cytotoxicity and cellular uptake of CDD in breast cancer cells.

3. Experimental

3.1. Materials

Medium viscosity sodium alginate of molecular weight 80,000-120,000 g/mol and low guluronic acid content (F_G = 0.39) was purchased from Sigma, St. Louis, MO, USA. Chitosan of molecular weight 83,000 g/mol and a degree of deacetylation of about 85% was purchased from Aquatic Nutrition Lab Co. Ltd., Samut Sakorn, Thailand. Pluronic F127 was supplied by BASF Chemical Company, Ludwigshafen, Germany. CDD was synthesized as described by Wichitnithad et al. (2011). Tetrahydrofuran (THF) was of HPLC grade and other chemicals were of analytical grade.

3.2. Cell culture

Human Caucasian breast adenocarcinoma MDA-MB-231 cells were obtained from the American Type Culture Collection (ATCC, Manassas, VA). Briefly, 3×10^3 cells/200 ml/well were seeded in 96-well plates with Dulbecco's Modified Eagle's Medium (DMEM) supplemented with 10% (v/v) heat inactivated fetal bovine serum (FBS) and 1% (v/v) penicillin-streptomycin solution. Cells were incubated at 37 °C in a saturated humid atmosphere containing 95% air and 5% CO_2.

3.3. Preparation of CDD-loaded nanoparticles

A sodium alginate solution was prepared by dissolution in ultrapure water (Milli-Q; Millipore, Molsheim, France) and its pH was adjusted to 4.9 with 1% (v/v) acetic acid solution. A chitosan solution was prepared by dissolution in 1% (v/v) acetic acid solution following by pH adjustment to 4.6 with 4% NaOH solution. All of solutions were filtered via a 0.45-mm cellulose acetate membrane filter for removal of impurity. CDD-loaded nanoparticles were prepared using o/w emulsification followed by ionotropic gelation as described by Lertsutthiwong et al. (2009) with modifications. Briefly, 1 ml of acetonic CDD solution at an appropriate concentration was added dropwise into 20 ml of sodium alginate solution (0.6 mg/ml) containing Pluronic F127 as a stabilizer using an automatic syringe pump (NE 100, New Era, Pump System Inc. USA) at a rate of 20 ml/h. After continuous magnetic stirring at 1,000 rpm for 10 min, 4 ml of $CaCl_2$ solution (0.67 mg/ml) was added dropwise to the resulting o/w emulsion and continuously stirred for 30 min. After sonication at a frequency of 45 kHz and sonic power 80 W for 15 min using an ultrasonic bath (CP 230, Crest Ultrasonics Corp., Ewing, NJ, USA), 4 ml of chitosan solution was added to the resulting calcium/alginate pre-gel and stirred for 30 min. The nanoparticle suspensions were equilibrated overnight in the dark to allow formation of a uniform particle size. The CDD-loaded nanoparticles were finally obtained as a dispersion in aqueous solution.

3.4. Experimental design

Previous work indicated that formulation parameters such as chitosan/alginate mass ratio, Pluronic F127 and CDD concentrations were the main factors affecting the characteristics of CDD-loaded nanoparticles in terms of particle size, size distribution, encapsulation efficiency and loading capacity (Bhunchu et al. 2015). Therefore, Box-Behnken design was used to optimize the formulation parameters and evaluate the main effects, interaction effects and quadratic effects of the formulation factors on the particle size (Y_1), zeta potential (Y_2), encapsulation efficiency percentage (Y_3) and loading capacity percentage (Y_4) of CDD-loaded nanoparticles. Chopra et al. (2007) suggested that the Box-Behnken model requires fewer experimental runs than the central composite design model. The cubic design is characterized by a set of points lying at the midpoint of each edge of a multidimensional cube and center point replicates (n = 3), with the 'missing corners' helping to avoid combined factor extremes. Box-Behnken design provides a suitable means of optimizing and testing for a wide range of applications in the food and pharmaceutical industries (Amenaghawon et al. 2013).

3.5. Characterization of CDD-loaded nanoparticles

Particles size, polydispersity index (PDI) and zeta potential were measured using a Zetasizer model Nano-ZS (Malvern Instruments, UK). The measurement of the particle size and PDI was performed by dynamic light scattering with an angle detection of 90 ° and the temperature was controlled at 25 °C. The zeta potential was characterized by laser doppler electrophoresis technique and its value was calculated by Smoluchowski's model. The morphology of the CDD-loaded nanoparticles was visualized by transmission electron microscopy (TEM, model H-9500; Hitachi High Technology America Inc., USA).

The amount of CDD in nanoparticles was assayed by HPLC according to USP36-NF31 with some modification. The CDD-loaded nanoparticles were separated from the aqueous medium by ultracentrifugation at 45,000 rpm at 4 °C for 1 h and lyophilized at -50 °C for 24 h to obtain powdered nanoparticles. The lyophilized nanoparticles were then extracted in 1 ml of the mobile phase of 1 mg/ml citric acid in water and tetrahydrofuran (40:60, v/v) under vortex for 1 min, followed by centrifugation at 14,000 rpm for 30 min. The supernatant was then collected for analysis. The 20-ml sample was injected onto the HA 166 (C18, 4.6×150 mm, 5 mm) column, which was maintained at 40 °C. The elution was isocratic at a flow rate of 1.0 ml/min and detection was carried out at 400 nm. The total chromatographic analysis time per sample was 4 min, with CDD eluting at a retention time of 3.38 min. The encapsulation efficiency and loading capacity were calculated as follows:

$$\text{Encapsulation efficiency (\%)} = \frac{\text{total amount of CDD in the nanoparticles} \times 100}{\text{total amount of CDD initially added in the formulation}} \quad (5)$$

$$\text{Loading capacity (\%)} = \frac{\text{total amount of CDD in the nanoparticles} \times 100}{\text{total dry mass of nanoparticles}} \quad (6)$$

Thermal properties of nanoparticles were analyzed using a thermogravimetric analyzer (TGA, model STA 409 PG/4/G Luxx, Netzsch, USA) using a heating rate of 5 °C/min from 30 to 800°C under a nitrogen atmosphere with a flow rate of 10 ml/min. The interaction of CDD and excipients was analyzed by Fourier transform infrared spectrometry (FT-IR, model ALPHA; Bruker, Philadelphia, PA, USA) in ATR mode. The analysis was carried out in spectral transmittance mode at 4000-400 cm^{-1} with a speed of 4 mm/s and resolution of 2 cm^{-1}. The physical state of CDD in the nanoparticle matrix was determined by wide-angle X-ray diffraction (XRD, model PW3710; Philips, The Netherlands). Samples were irradiated with monochromatized CuKα radiation (1.542 Å) and analyzed at 2θ range of 20-60 ° at a scanning speed of 0.2° 2q/step. The detector was operated at a voltage of 40 kV and a current of 30 mA.

3.6. Data analysis and model validation

ANOVA was used for statistical analysis of the polynomial equations generated by Design Expert® software. A total of 15 experimental runs in triplicate at center points were generated by Box-Behnken design. The mathematic model for mixture design includes linear, interaction and quadratic components. The best fitting mathematic model was selected based on several statistical parameters, including the multiple correlation coefficient (R^2), adjusted R^2, predicted R^2, standard deviation (SD), coefficient of variation (CV) and the predicted residual sum of squares (PRESS) calculated in Design Expert® software. PRESS and CV indicate how well the model fits the data, and should be small for the chosen model relative to other models (Kim et al. 2007). Three dimensional response surface plots were generated in Design Expert® software using an intensive grid search over the whole experimental region. The optimal formulation was selected to validate the chosen experimental domain and polynomial equations, and was prepared and evaluated for various response properties. The resultant experimental values of the responses were compared with the predicted values to calculate the % prediction error. Linear regression plots between actual and predicted values of the responses were produced using MS-Excel 2013.

3.7. In vitro cytotoxicity assay

The cytotoxicity of CDD in MDA-MB-231 cells was determined using a 3-(4,5-dimethylthiazol-2-yl)-2,5-diphenyl tetrazolium bromide (MTT) based colorimetric assay. This method is used to analyze the cytotoxicity of bioactive compounds based on the capacity of living cells to metabolize the yellow water soluble substrate MTT to an insoluble dark blue formazan product (Vega-Avila and Pugsley 2011). The MTT assay was carried out using the method described by Umthong et al. (2011). MDA-MB-231 cells were cultured in DMEM supplemented with 10% (v/v) heat inactivated fetal bovine serum (FBS) and 1% (v/v) antibiotic penicillin-streptomycin solution and incubated at 37 °C in a humid atmosphere containing 95% air and 5% CO_2 until the cells reached 80% confluence. The cells were seeded in 96-well plates at 3×10^3 cells/well and incubated in the same atmosphere for 24 h. The cells were then washed with DMEM and treated with 200 µl of fresh DMEM containing a CDD-loaded nanoparticle suspension, blank chitosan/alginate nanoparticles or free CDD at drug concentrations ranging from 0.3-5 µg/ml and incubated for 72 h. Dimethyl sulfoxide (DMSO) and blank nanoparticles were used as positive and negative controls, respectively. MTT was then added to each well and incubated for 4 h, followed by removal of the solution. DMSO was added and thoroughly mixed for 10 min before measurement of absorbance at 540 nm using a microplate reader (Molecular Devices, USA). Cell growth without nanoparticles was evaluated as a control. Cell viability was calculated as follows:

$$\text{Cell viability (\%)} = \frac{OD_{sample}}{OD_{control}} \times 100 \quad (7)$$

The results are shown as the half maximal inhibitory concentration (IC_{50}), which is the concentration of sample required to kill 50% of the cancer cells compared with the negative control.

3.8. In vitro cellular uptake

MDA-MB-231 cells were cultured in 96-well plates at 3×10^3 cells/well at 37 °C for 24 h. DMEM was then removed from each well. The cells were washed with 200 µl of DMEM and equilibrated for 1 h in an incubator at 37 °C. A 2-µl sample of free CDD, blank chitosan/alginate nanoparticles or CDD-loaded nanoparticles was introduced into each well in 200 µl of DMEM and incubated for 72 h. The cells were then washed with 0.01 M phosphate-buffered solution (pH 7.4) to remove excess nanoparticles or free CDD, followed by addition of fresh PBS buffer. The cells were then visualized by confocal laser scanning microscopy (Nikon, D-ECLIPSE C1, Japan) using a green channel with excitation at 400 nm and emission at 470 nm. Images were processed with the aid of Nikon software. Cellular uptake was expressed as the fluorescence intensity associated with CDD-loaded nanoparticles versus the fluorescence intensity associated with free CDD.

3.9. Stability study

The stability of the nanoparticle suspension was determined based on ASEAN guidelines (2005) for stability of drug products. The CDD-loaded nanoparticle suspension was stored in amber bottles in the dark at 4 °C and 25 °C for 3 months. The particle size, zeta potential, encapsulation efficiency and loading capacity of the nanoparticle suspensions were determined at specific time intervals.

Acknowledgments: The authors express their gratitude to the Ratchadaphiseksomphot Endowment Fund of Chulalongkorn University (RES560530014-AM), the 90th Anniversary of Chulalongkorn University Fund and Graduate School of Chulalongkorn University for providing research funds. We also thank Dr. Ian S. Haworth (University of Southern California) for his comments on the manuscript.

Conflicts of interest: None declared.

References

Abdelwahed W, Degobert G, Stainmesse S, Fessi H (2006) Freeze-drying of nanoparticles: Formulation, process and storage considerations. Adv Drug Deliv Rev 58: 1688-1713.

Ali A, Sinha K (2014) Exploring the opportunities and challenges in nanotechnology innovation in India. JSSPI 2: 227-251.

Amenaghawon NA, Nwaru KI, Aisien FA, Ogbeide SE, Okieimen CO (2013) Application of Box-Behnken design for the optimization of citric acid production from corn starch using *Aspergillus niger.* Br. Biotechnol J 3: 236-245.

Anand P, Kunnumakkara AB, Newman RA, Aggarwal BB (2007) Bioavailability of curcumin: problems and promises. Mol Pharm 4: 807-818.

Araujo V, Gamboa A, Caro N, Abugoch L, Gotteland M, Valenzuela F, Merchant HA, Basit AW, Tapia C (2013) Release of prednisolone and inulin from a new calcium-alginate chitosan-coated matrix system for colonic delivery. J Pharm Sci 102: 2748-2759.

Arora S, Gupta S, Narang RK, Budhiraja RD (2011) Amoxicillin loaded chitosan-alginate polyelectrolyte complex nanoparticles as mucopenetrating delivery system *for H. pylori.* Sci Pharm 79: 673-694.

Azevedo MA, Bourbon AI, Vicente AA, Cerqueira MA (2014) Alginate/chitosan nanoparticles for encapsulation and controlled release of vitamin B_2. Int J Biol Macromol 71: 141-146.

Bhunchu S, Rojsitthisak P (2014) Biopolymeric alginate-chitosan nanoparticles as drug delivery carriers for cancer therapy. Pharmazie 69: 563-570.

Bhunchu S, Rojsitthisak P, Rojsitthisak P (2015) Effects of preparation parameters on the characteristics of chitosan-alginate nanoparticles containing curcumin diethyl disuccinate. J Drug Deliv Sci Technol 28: 64-72.

Bisht S, Feldmann G, Soni S, Ravi R, Karikar C, Maitra A, Maitra A (2007) Polymeric nanoparticle-encapsulated curcumin ("nanocurcumin"): a novel strategy for human cancer therapy. J Nanobiotechnol 5: 1-18.
Chopra S, Patil GV, Motwani SK (2007) Release modulating hydrophilic matrix systems of losartan potassium: Optimization of formulation using statistical experimental design. Eur J Pharm Biopharm 66: 73-82.
Chuah LH, Roberts CJ, Billa N, Abdullah S, Rosli R (2014) Cellular uptake and anticancer effects of mucoadhesive curcumin-containing chitosan nanoparticles. Colloids Surf, B 116: 228-236.
Cousins M, Adelberg J, Chen F, Rieck J (2007) Antioxidant capacity of fresh and dried rhizomes from four clones of turmeric (*Curcuma longa* L.) grown *in vitro.* Indian Crops Prod 25: 129-135.
De S, Robinson D (2003) Polymer relationships during preparation of chitosan-alginate and poly-L-lysine-alginate nanospheres. J Control Release 89: 101-112.
Ghalandarlaki N, Alizadeh AM, Ashkani-Esfahani S (2014) Nanotechnology-applied curcumin for different diseases therapy. Biomed Res, Int Article ID 394264.
Gomathi T, Govindarajan C, Maximas H. Rose HRMH, Sudha PN, Mohamed Imran PK, Venkatesan J, Kim SK (2014) Studies on drug-polymer interaction, *in vitro* release and cytotoxicity from chitosan particles excipient. Int J Pharm 468: 214-222.
Kharia AA, Singhai AK, Verma R (2012) Formulaiton and evaluation of polymeric nanoparticles of an antiviral drug for gastroretention. Int J Pharm Sci Nanotech 4: 1557-1562.
Kim MS, Kim JS, You YH, Park HJ, Lee S, Park JS, Woo JS, Hwang SJ (2007) Development and optimization of a novel oral controlled delivery system for tamsulosin hydrochloride using response surface methodology. Int J Pharm 341: 97-104.
Kim S, Fernandes MM, Matamá T, Loureiro A, Gomes AC, Cavaco-Paulo A (2013) Chitosan-lignosulfonates sono-chemically prepared nanoparticles: Characterization and potential applications. Colloids Surf B Biointerfaces 103: 1-8.
Kunwar A, Barik A, Mishra B, Rathinasamy K, Pandey R, Priyadarsini KI (2008) Quantitative cellular uptake, localization and cytotoxicity of curcumin in normal and tumor cells. Biochim Biophys Acta 1780: 673-679.
Lertsutthiwong P, Noomun K, Jongaroonngamsang N, Rojsitthisak P, Nimmannit U (2008) Preparation of alginate nanocapsules containing turmeric oil. Carbohydr Polym 74: 209-214.
Lertsutthiwong P, Rojsitthisak P, Nimmannit U (2009) Preparation of turmeric oil-loaded chitosan-alginate biopolymeric nanocapsules. Mater Sci Eng C 29: 856-860.
Lertsutthiwong P, Haworth IS, Rojsitthisak P (2010) Alginate: A promising polysaccharide for delivery of essential oils. In: Ito R, Matsuo Y (ed.) Handbook of carbohydrate polymers: development, properties and applications. Nova Science Publishers, New York, p. 621-638.
Lertsutthiwong P, Rojsitthisak P (2011) Chitosan-alginate nanocapsules for encapsulation of turmeric oil. Pharmazie 66: 911-915.
Li X, Kong X, Shi S, Zheng X, Guo G, Wei Y, Qian Z (2008) Preparation of alginate coated chitosan microparticles for vaccine delivery. BMC Biotechnol 8: 89.
Motwani SK, Chopra S, Talegaonkar S, Kohli K, Ahmad FJ, Khar RK (2008) Chitosan-sodium alginate nanoparticles as submicroscopic reservoirs for ocular delivery: Formulation, optimization and *in vitro* characterization. Eur J Pharm Biopharm 68: 513-525.
Paula HCB, Sombra FM, Abreu FOMS, de Paula RCM (2010) *Lippia sidoides* essential oil encapsulation by angico gum/chitosan nanoparticles. J Braz Chem Soc 21: 2359-2366.
Ranjan AP, Mukerjee A, Helson L, Vishwanatha JK (2012) Scale up, optimization and stability analysis of Curcumin C3 complex-loaded nanoparticles for cancer therapy. J Nanobiotechnol 10: 38.
Sankalia MG, Mashru RC, Sankalia JM, Sutariya VB (2007) Reversed chitosan-alginate polyelectrolyte complex for stability improvement of alpha-amylase: optimization and physicochemical characterization. Eur J Pharm Biopharm 65: 215-232.
Sarmento B, Ribeiro AJ, Veiga F, Ferreira DC, Neufeld RJ (2007) Insulin-loaded nanoparticles are prepared by alginate ionotropic pre-gelation followed by chitosan polyelectrolyte complexation. J Nanosci Nanotechnol 7: 2833-2841.
Segurola J, Allen NS, Edge M, Mc Mohan A (1999) Design of eutectic photoinitiator blends for UV/visible curable acrylated printing inks and coatings. Prog Org Coat 37: 23-37.
Sekhon BS (2010) Food nanotechnology-an overview. Nanotechnol Sci Appl 3: 1-15.
Sugama T, Cook M (2000) Poly(itaconic acid)-modified chitosan coatings for mitigating corrosion of aluminum substrates. Prog Org Coat 38: 79-87.
Sun J, Bi C, Chan HM, Sun S, Zhang Q, Zheng Y (2013) Curcumin-loaded solid lipid nanoparticles have prolonged in vitro antitumour activity, cellular uptake and improved in vivo bioavailability. Colloids. Surf. B 111: 367-375.
Ukil A, Maity S, Karmakar S, Datta N, Vedasiromoni JR, Das PK (2003) Curcumin, the major component of food flavour turmeric, reduces mucosal injury in trinitrobenzene sulphonic acid-induced colitis. Br. J Pharmacol 139: 209-218.
Umthong S, Phuwapraisirisan P, Puthong S, Chanchao C (2011) *In vitro* antiproliferative activity of partially purified Trigona laeviceps propolis from Thailand on human cancer cell lines. BMC Complement Altern Med 11: article 37
Vega-Avila E, Pugsley MK (2011) An Overview of Colorimetric Assay Methods Used to Assess Survival or Proliferation of Mammalian Cells. Proc West Pharmacol Soc 54: 10-14.
Wichitnithad W, Nimmannit U, Wacharasindhu S, Rojsitthisak P (2011) Synthesis, characterization and biological evaluation of succinate prodrugs of curcuminoids for colon cancer treatment. Molecules 16: 1888-1900.
Woitiski CB, Veiga F, Ribeiro A, Neufeld R (2009) Design for optimization of nanoparticles integrating biomaterials for orally dosed insulin. Eur J Pharm Biopharm 73:25-33
Yang R, Zhang S, Kong D, Gao X, Zhao Y, Wang Z (2012) Biodegradable polymer-curcumin conjugate micelles enhance the loading and delivery of low-potency curcumin. Pharm Res 29: 3512-3525.
Yang YT, Di Pasqua AJ, He W, Tsai T, Sueda K, Zhang Y, Jay M (2013) Preparation of alginate beads containing a prodrug of diethylenetriaminepentaacetic acid. Carbohydr Polym 92: 1915-1920.
Zhang Y, Wei W, Lv P, Wang L, Ma G (2011) Preparation and evaluation of alginate–chitosan microspheres for oral delivery of insulin. Eur J Pharm Biopharm 77: 11-19.